

Copper(I)-Catalyzed [2 + 2] Photocycloadditions with Tethered Linkers: Synthesis of Syn-Photodimers of Dicyclopentadienes

Elena Galoppini,^{*,†} Ravikrishna Chebolu,[†] Richard Gilardi,[‡] and Wei Zhang[†]

Department of Chemistry, Rutgers University, 73 Warren Street, Newark, New Jersey 07102, and Laboratory for the Structure of Matter, The Naval Research Laboratory, Washington DC 20375

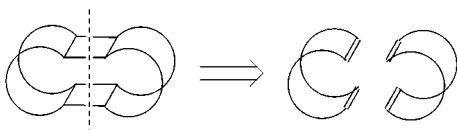
galoppin@andromeda.rutgers.edu

Received August 7, 2000

Cu(I)-catalyzed intramolecular photocycloadditions of diesters made of *endo*-dicyclopentadiene derivatives linked by the ester bonds with tethers are highly regio- and stereoselective and complete within hours, and the tethers can be easily cleaved afterward upon reduction with LiAlH₄. Irradiation of the diesters afforded a 1:1 mixture of the heretofore unknown *exo-cis-exo* dimer, originating from the (*R,S/S,R*) diastereomer of the diester and the *exo-trans-exo*, deriving from the (*R,R/S,S*) diastereomer. The intermolecular photodimerization yielded, instead, only *exo-trans-exo* isomers and side products after irradiation for several days. The role of the tether's length and structure on the course of the photocycloadditions was investigated, and it was observed that short tethers introduce considerable strain in the products' framework. Adamantyl-containing tethers provided the shortest reaction times and highest yields. X-ray diffraction analysis of an *exo-cis-exo* stereoisomer containing adamantane in the tether exhibited an unusually close approach between H atoms on the methylene bridges and a long C–C distance in the cyclobutane ring. A rearrangement induced by X-ray irradiation was observed in this molecule.

Introduction

Polycarbocyclic cage molecules, a class of organic compounds that has interested chemists for decades, might be deconstructed in numerous different retrosynthetic pathways. One of the simplest, that can be applied to many cage frameworks, is cleavage into two cyclic dienes "halves".¹



Dimerization of such cyclic dienes via syn-stereoselective [2 + 2] photocycloadditions may therefore open a direct route to a variety of new cage and ring molecules. The attempted syntheses of important cage molecules by dimerization of norbornenes,² norbornadienes,^{2a,3} dicyclopentadienes,^{2b} triquinacenes,⁴ and other polycyclic bridged alkenes^{1a,b,e} were all based on this concept. These efforts, however, involved intermolecular reactions that produced anti-fused dimers, Scheme 1A. A syn photocycloaddition would require the face-to-face alignment of the two reacting "halves" which, at least in theory, may

be accomplished with the aid of a tether. A cage-like structure could then be formed either in a single step or following a series of transformations, as illustrated in Scheme 1B.

This strategy was employed by Gleiter and Karcher for the synthesis of a cubane derivative: irradiation of a *syn*-tricyclo[4.2.0.0^{2,5}]octa-3,7-diene bridged by C₃ units led to a photocyclic ring closure not observed in the absence of the propane bridges.⁵ The use of tethers to link two molecules and perform a reaction intramolecularly is a strategy that is increasingly employed in a wide variety of organic reactions, including copper(I)-catalyzed [2 + 2] photocycloadditions.^{6,7} This methodology is especially practical when it uses "disposable" or "removable" tethers, often silicon- or oxygen-based, that can be cleaved after the reaction.⁸ The reaction rates are generally higher, because of the decreased entropic demands, and the reduction in the degrees of freedom of the unimo-

(2) (a) Arnold, D. R.; Trecker, D. J.; Whipple, E. B. *J. Am. Chem. Soc.* **1965**, *87*, 2596. (b) Salomon, R. G.; Kochi, J. K. *J. Am. Chem. Soc.* **1974**, *96*, 1137.

(3) (a) Marchand, A. P.; Earlywine, A. D.; Heeg, M. J. *J. Org. Chem.* **1986**, *51*, 4096. (b) Acton, N.; Roth, R. J.; Katz, T. J.; Frank, J. K.; Maier, C. A.; Paul, I. C. *J. Am. Chem. Soc.* **1972**, *94*, 5446. (c) Chow, T. J.; Chao, Y.-S.; Liu, L.-K. *J. Am. Chem. Soc.* **1987**, *109*, 797. (d) Chow, T. J.; Liu, L.-K.; Chao, Y.-S. *J. Chem. Soc., Chem. Commun.* **1985**, 700.

(4) Coddling, P. W.; Kerr, K. A.; Oudeman, A.; Soresen, T. S. *J. Organomet. Chem.* **1982**, *232*, 193.

(5) Gleiter, R.; Karcher, M. *Angew. Chem., Int. Ed. Engl.* **1988**, *27*, 840.

(6) The classification "Cu(I)-catalyzed [2 + 2] photocycloaddition" is commonly used, but it does not necessarily imply that these are concerted reactions which strictly follow the Woodward–Hoffmann orbital symmetry rules.

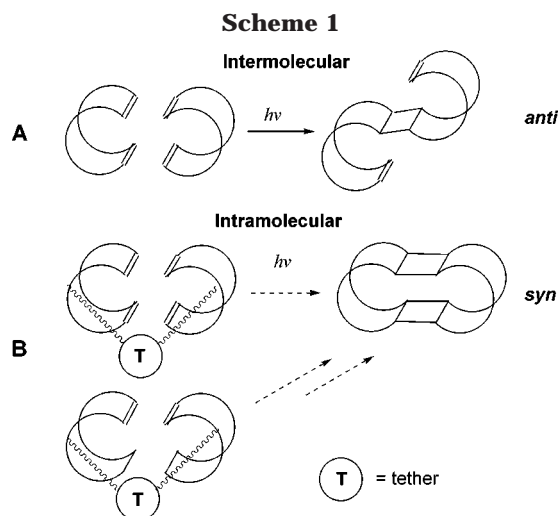
(7) For reviews on this class of reactions, see: (a) Langer K.; Mattay, J. In *CRC Handbook of Organic Photochemistry and Photobiology*; Horspool, W. M., Song, P.-S., Eds.; CRC Press: Boca Raton, 1995; pp 84–101. (b) Salomon, R. G. *Tetrahedron* **1986**, *42*, 5753–5839.

(8) For a recent review, see: Gauthier, D. R.; Zandi, K. S.; Shea, K. *J. Tetrahedron* **1998**, *54*, 2289.

[†] Rutgers University.

[‡] The Naval Research Laboratory.

(1) For reviews mentioning this approach, see: (a) Mehta, G.; Padma S. In *Carbocyclic Cage Compounds*; Osawa E., Yonemitsu, O., Eds.; VCH: New York, 1994; pp 183–215. (b) Mehta, G. In *Strain and its Implications in Organic Synthesis*; de Meijere, A., Blechert, S., Eds.; NATO ASI Ser., *273*, 1989; pp 269–281. (c) Hopf, H. *Classics in Hydrocarbon Chemistry*; Wiley-VCH: Weinheim, 2000; Chapter 4, pp 41–51 and Chapter 5, pp 53–80. (d) Marchand, A. P. In *Second Supplements to the 2nd Edition of Rodd's Chemistry of Carbon Compounds*; Sainsbury, M., Ed.; Elsevier Science: Amsterdam, 1994; Vol. II, pp 277–329. (e) Forman, M. A.; Dailey, W. P. *Org. Prep. Proc. Int.* **1994**, *26*, 291.



lecular transition state results in higher regio- and stereoselectivity. Isomers that are not observed in the corresponding intermolecular reactions can often be synthesized only with this method. For instance, the [2 + 2] photocycloaddition of dihydropyridones, coumarins, maleimides and numerous other molecules occurred with syn stereoselectivity when performed intramolecularly using tethered linkers.⁹ In view of these results, we have applied this methodology to polycyclic bridged alkenes, aimed at the synthesis of syn-fused dimers. In a preliminary study, we showed that linking two *endo*-dicyclopentadiene derivatives with a tether increased the efficiency of the photocycloaddition reaction.¹⁰ Herein, we report a comparison between several substrates with different tethers and expand the study of the reaction stereoselectivity.

Results and Discussion

Synthesis of Tethered Diesters. Diesters **3a–f** shown in Scheme 2 served as the prototypes to test this strategy. Each diester consists of two *endo*-dicyclopentadiene moieties linked by a tether containing either an alkyl chain or an adamantyl spacer. To reduce the number of photocycloaddition products, and to simplify the analysis of the stereoselectivity of the reaction, the cyclopentene double bond in each moiety was reduced and only the norbornyl double bond was left available for the photocycloaddition.¹¹ Diesters **3a–f** were obtained in 70–85% yield in one step from alcohol **1**¹² and diacyl chlorides **2a–f**.

(9) (a) Comins, D. L.; Lee, Y. S.; Boyle, P. D. *Tetrahedron Lett.* **1998**, *39*, 187. (b) Hertel, R.; Mattay J.; Runsink, J. *J. Am. Chem. Soc.* **1991**, *113*, 657. (c) Garner, P.; Cox, P. B.; Anderson, J. T.; Protasiewicz J.; Zaniewski, R. *J. Org. Chem.* **1997**, *62*, 493. (d) De Schryver, F. C.; Boens N.; Put, J. In *Advances in Photochemistry*; Pitts, J. N., Hammond G. R., Collnick, K., Eds.; John Wiley & Sons: New York, 1977; Vol. 10, pp 359–464.

(10) Chebolu, R.; Zhang, W.; Galoppini, E.; Gilardi, R. *Tetrahedron Lett.* **2000**, *41*, 2831.

(11) The strained "norbornyl" double bond is the most reactive and usually the "cyclopentenyl" double bond does not participate in the photocycloaddition. However, depending on the reaction conditions, there are two competing reactions that involve the cyclopentene moiety: (a) Photopolymerization reactions, which can be avoided by working with highly diluted solutions; (b) The intramolecular [2 + 2] photocycloaddition between the norbornyl and the cyclopentenyl double bond within each dicyclopentadiene moiety, leading to the formation of bishomocubane. Although this competing reaction does not occur in THF in the presence of Cu(I),^{2b} we did isolate a small amount of bishomocubane products when the photocycloaddition was slow and the dicyclopentadiene diesters were irradiated for many hours.

(12) Dilling W. L.; Plepys, R. A. *J. Org. Chem.* **1970**, *35*, 2971.

The length of the alkyl chain tethers was varied incrementally to study the effect on the reaction's rate and stereochemistry, while the purpose of the adamantyl spacer was to make the linker more rigid.¹³ Since **1** was prepared in racemic form,^{14,15} each diester was a mixture of two diastereomeric pairs, (*R,R/S,S*) and (*R,S/S,R*). The photocycloadditions were performed on this mixture, except for **3d** and **3e**, where in each case the (*R,R/S,S*) pair was isolated in pure form.

As the Cu(I) source we used CuOTf, which is often preferred to copper halide salts in this type of reactions because it is soluble in organic solvents and is photostable. Cu(I) can coordinate to alkenes to form 1:1 or 1:2 Cu(I)-olefin complexes that exhibit UV absorption bands (metal-to-ligand or ligand-to-metal charge-transfer bands) in the range of 250–300 nm. According to the most generally accepted mechanism, excitation of these bands in the 1:2 complexes is the first step of a process that leads to the photocycloaddition products.⁷ Depending on the structure of the alkene and the copper salt employed, the reaction can proceed through different mechanisms: the photocycloaddition can occur via concerted, orbital-symmetry allowed photochemical cycloadditions as well as sequential pathways involving radical or cationic copper alkyl intermediates.⁷

Intermolecular Photocycloaddition. For a comparison, we first studied the intermolecular photocycloaddition of untethered **4**, Scheme 3.¹⁰ As had been observed with other polycyclic bridged alkenes, including *endo*-dicyclopentadiene,^{2b} irradiation of **4** in THF in the presence of a catalytic amount of CuOTf¹⁶ for several days produced two *exo-trans-exo* dimers, **5** and **6**, in 62% yield along with traces of other dimers (GC/MS) and decomposition products. Dimers **5** and **6** are diastereomers derived from the photocycloaddition between two opposite and identical enantiomers of **4**, respectively, and were formed in 1:1 ratio. The configuration of each isolated dimer was deduced through single-crystal X-ray structure determinations (see the Supporting Information).

Intramolecular Photocycloadditions. The intramolecular [2 + 2] photocycloadditions between tethered diesters **3a–f** were also performed in THF and in the presence of a catalytic amount of CuOTf.¹⁶ In most cases, these photocycloadditions were complete in a few hours, whereas the corresponding intermolecular reactions required days. More interestingly, the photocycloaddition afforded a completely different set of products because of the constraints imposed by the tethers. For instance, stereoisomers having the alcohol groups on opposite sides, as in **5**, did not form. In all cases, only two isomers were recovered, the *exo-trans-exo-7* and the *exo-cis-exo-8* in 1:1 ratio and 70–80% yields, Scheme 4.¹⁷ The synthesis of the *exo-cis-exo*-dicyclopentadiene dimers was unprecedented and demonstrates the usefulness of the tethers.

The photocycloaddition is highly stereospecific: the *exo-trans-exo* isomers **7** are formed from the (*R,R/S,S*)

(13) In addition, the adamantane frame is transparent in the region of the UV absorption spectrum where Cu(I)-olefin complexes absorb.

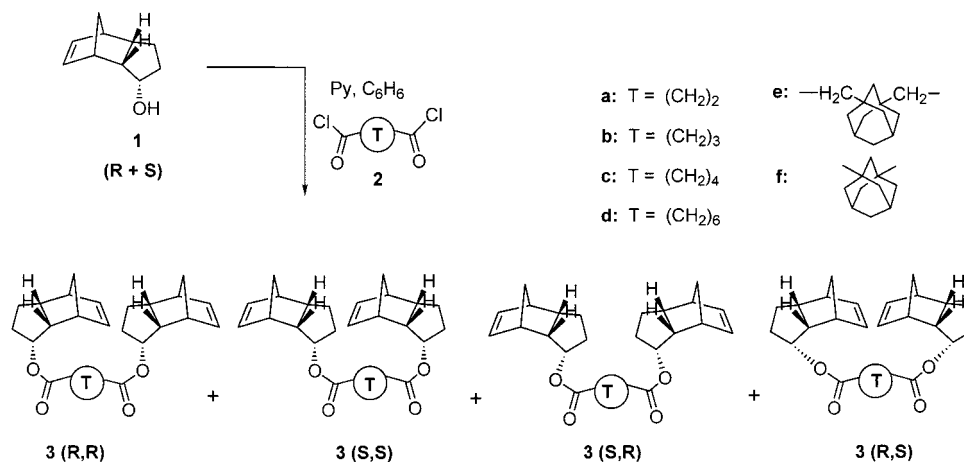
(14) The (*R*) and (*S*) designations refer to the alcohol stereocenter of **1**.

(15) The resolution of **1** was not performed, because it would result in the diastereoselective synthesis of the (*R,R*) or the (*S,S*) diester, and each is the precursor of the less interesting *exo-trans-exo* product.

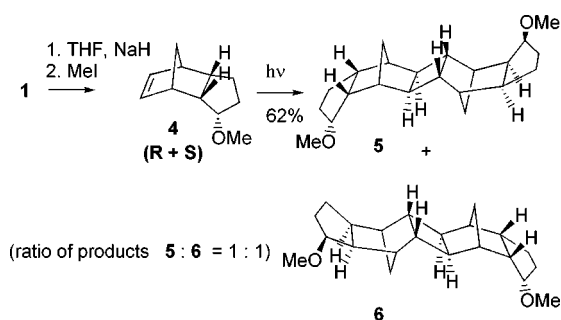
(16) The photocycloaddition did not occur in the absence of CuOTf.

(17) Products having *endo-cis-endo* geometry were not observed. Ab initio calculations using Gaussian 98 performed at 6-31G** level on structures optimized using PM3 (as well as simple molecular models) clearly show that these molecules would be highly strained.

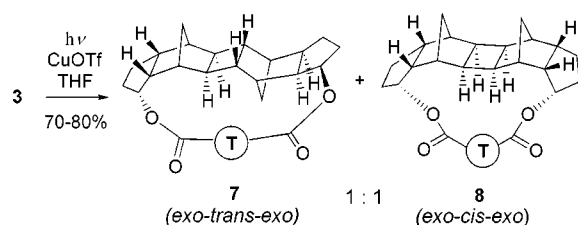
Scheme 2



Scheme 3



Scheme 4



diastereomers of **3**, and the *exo-cis-exo* isomers **8** derive from the (*R,S/S,R*). Therefore, either anti- or, more interestingly, syn-fused products can be selectively obtained by starting with the appropriate diastereomer of the diester.¹⁵ We found, however, that it is easier to separate the mixture of **7** and **8** than a diastereomeric mixture of **3**. The configuration of each isolated stereoisomer was determined by single-crystal X-ray analysis or NMR.

The crystal structure of *exo-trans-exo-7d*¹⁰ showed diastereomer (*R,R*) and two molecules of (*S,S*) differing in their torsion angles along the C6 tether-chain. The crystal structure of *exo-cis-exo 8f*, shown in Figure 1, exhibited several unusual features, including a very close approach (1.74 Å) between H atoms on the methylene bridges,¹⁸ C10 and C17, and a long C12–C15 distance^{19,20} in the cyclobutane ring (1.68(1) Å). The distortion of the central cyclobutane ring (C13–C14 = 1.534(9) Å; C12–C15 = 1.677(7) Å; C13–C12 = 1.547(8) Å; C14–C15 = 1.530(8) Å) suggests that the short semirigid tether and the very close approach between the methylene bridges introduce a considerable amount of strain in the molecules' framework.

The collection and analysis of the X-ray data from **8f** show the occurrence of an X-ray-initiated rearrangement of the strained ring system. This rearrangement does not

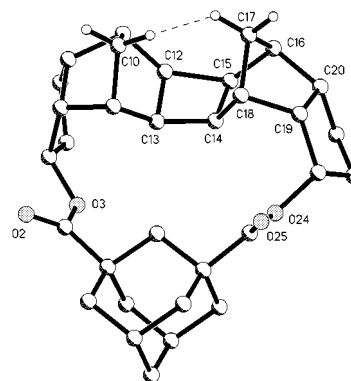


Figure 1. X-ray structure of **8f**. The *cis*-fused ring system in **8f** is distorted, displaying an overall torsion that removes left-right symmetry, and a long C12–C15 bond in the cyclobutane ring (see text).

disrupt the crystal lattice and leads to a second structural isomer in a fraction of the unit cells of the crystal.²¹ Electron density maps show a spatial average over all unit cells, so we see a superposition of the two isomers, with **8f** as the dominant species.

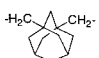

Role of the Structure of the Tether. To understand how the structure of the tether influences the course of the photocycloaddition we used several linkers differing in length and rigidity. In general, we observed that the efficiency of the reaction depended dramatically on these two parameters, while the stereoselectivity did not change. The effect of the tether's length is shown in Table 1, **3a–d**: reaction rates increase as the aliphatic chains become longer. The yields also improved with shorter reaction times, as prolonged irradiation leads to decomposition products. A possible explanation for the trend shown in Table 1 may be found in the strain energy content of the products. A correlation between calculated strain energy values with the number of methylenic units (CH₂)_{*n*} (*n* = 0–6) in the alkyl chain-tethered *exo-trans-*

(18) The H atoms in **8f** were placed in ideal sp³ locations. A similar nonbonded distance, 1.61 Å, was reported in a polycycle by: Warner, P. M.; LaRose, R. C.; Palmer, R. F.; Lee, C.-M.; Ross, D. O.; Clardy, J. C. *J. Am. Chem. Soc.* **1975**, *97*, 5507.

(19) This result may be affected by the presence of **9** but it is not unprecedented: a cyclobutane ring distance of 1.720(4) Å is reported in: Toda, F.; Tanaka, K.; Stein, Z.; Goldberg, I. *Acta Crystallogr.* **1996**, *C52*, 177.

(20) For a review on long C–C single bonds in strained molecules: Osawa, E.; Kanematsu, K. In *Molecular Structure and Energetics*; Liebman, J. F., Greenberg, A., Eds.; VCH: Deerfield Beach, FL, 1986; Vol. 3, pp 329–369.

Table 1. Reaction Times^a and Yields^b for the Photocycloaddition Reactions of 3a–f

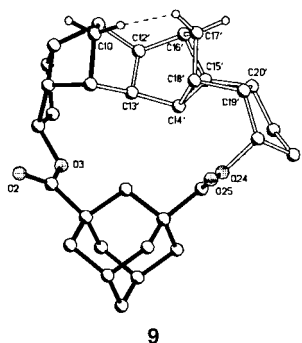
Diester	Tether	Time (h)	Yield (%)
3a	-(CH ₂) ₂ -	48	traces
3b	-(CH ₂) ₃ -	27	62
3c	-(CH ₂) ₄ -	14	76
3d	-(CH ₂) ₆ -	3	75 ^c
3e		3	80 ^c
3f		3	80

^a Time required for disappearance of olefinic protons in ¹H NMR spectra. ^b Isolated yield of **7** and **8**. ^c Isolated yield of **7**.²⁸

exo product series indicates that the strain decreases as *n* increases.^{22,23} Compound **6**, which has no tether (*n* = 0), is the least strained photocycloaddition product.

An additional indication that short tethers introduce tension in the molecules' frameworks derives from experimental and calculated values of C–C bond distances in the central cyclobutane ring of exo-trans-exo products, Table 2.²⁴ These data show that the central cyclobutane ring is not symmetrical in the tethered molecules. Specifically, C–C bond distances obtained from the X-ray crystallographic data analysis show that in **7d**¹⁰ and **7e** (see the Supporting Information) the cyclobutane bond on the side of the tether (labeled as **a** in Table 2) is slightly shorter than the one on the opposite side (bond **b**) while in **5** and **6**, which do not contain a tether, **a** and **b** are identical. We examined only exo-trans-exo products to correlate the tethers' length with the strain energy because this association can be established more clearly in the trans compounds, which lack the additional strain due to close contacts between the methylene bridges as seen in the exo-cis-exo products.

(21) A possible structure for the rearrangement product is **9**. This was suggested by the final difference maps taken from a crystal that had been irradiated for 4 days, showing the appearance of two peaks (C15' and C16') in the vicinity of C15 and C16, and by the observation that atoms C12 to C23 have counterparts in both **8f** and the rearranged product.



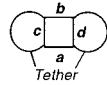
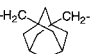

Additional features in favor of **9** are the observation that the rearranged product is a structural isomer of **8f**, the fact only two bonds (C12–C15 and C16–C20) need be "disconnected" and "reconnected" to obtain **9** from **8f**, and preliminary calculations,²² indicating that the replacement of the four-membered ring with a cyclopentane would relieve strain in the molecule. However, we currently do not have any additional experimental evidence supporting **9**.

(22) Strain energy values for **8f** (176 kcal/mol) and **9** (122 kcal/mol) and for the alkyl chain-tethered exo-trans-exo product series were calculated using single-point molecular mechanics calculations (SYBYL) using PC Spartan Pro, Wavefunction, Inc.

(23) Ab initio calculations of the final photocycloaddition products using Gaussian 98 performed at 6-31G** level on structures optimized using PM3 are in progress.

(24) The calculated bond lengths reported in Table 2 were obtained from structures minimized using semiempirical calculations (AM1 and PM3) using PC Spartan Pro, Wavefunction, Inc.

Table 2. Experimental^a and Calculated^b (Shown in Italics) Bond Lengths (Å) in the Cyclobutane Ring of Exo-Trans-Exo Products

Product	Tether				
		a	b	c	d
5	-	1.568(2)	1.568(2)	1.551(2)	1.551(2)
6	-	1.551(2)	1.548(2)	1.570(2)	1.574(2)
		<i>1.54</i>	<i>1.54</i>	<i>1.59</i>	<i>1.59</i>
7a	-(CH ₂) ₂ -	1.50	1.60	1.57	1.57
7b	-(CH ₂) ₃ -	1.50	1.58	1.58	1.58
7c	-(CH ₂) ₄ -	1.52	1.57	1.58	1.58
7d	-(CH ₂) ₆ -	1.543(9)	1.563(9)	1.576(8)	1.580(8)
		<i>1.54</i>	<i>1.54</i>	<i>1.59</i>	<i>1.59</i>
7e		1.540(4)	1.558(5)	1.572(4)	1.567(4)
		<i>1.52</i>	<i>1.56</i>	<i>1.59</i>	<i>1.59</i>
7f		1.50	1.59	1.58	1.58

^a From X-ray crystallographic data. ^b From semiempirical calculations (AM1 and PM3).²⁴

Finally, the rigidity of the tether introduced by the adamantyl groups also plays a role in this reaction, as suggested by the difference in rates of products formation between **3b** and **3f**, Table 1. Both diesters have the two reacting moieties separated by a three-carbon atom spacer, but the rate of photocycloaddition for **3f**, in which the spacer incorporates a rigid adamantane frame, is nine times faster than that of **3b**. One possible explanation is that conformational restrictions introduced by the semirigid 1,3-adamantyl spacer favor the formation of a Cu(I) complex bridging the two alkenes in the transition state. CuOTf shows a strong tendency to form 1:2 Cu(I)–olefin complexes,^{7a} where the metal bridges two olefins. In particular, this has been observed for dicyclopentadiene, where only the more strained "norbornyl" double bond coordinates with Cu(I), and for norbornene.²⁵ In our case, however, it is not straightforward to assume the same kind of structure for the Cu(I)-diester **3** complexes. The ester group could play a role in coordinating with the metal and the bulky tethers may introduce steric factors not present in unsubstituted dicyclopentadiene.

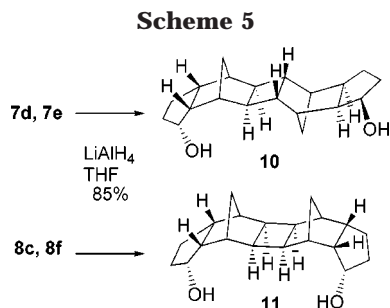
Although our observations on the role of the linker are limited to experiments with one kind of polycyclic alkene, we believe that the use of adamantyl tethers will be useful in future studies. In addition to more efficient photocycloadditions, the isolation and characterization of all adamantyl-containing compounds were considerably easier than that of compounds with aliphatic chains: the separation of **7** and **8** on silica gel was increased; **8f** and **7e** formed crystals of good quality,²⁶ and the aliphatic region in the ¹H NMR spectra was somewhat simplified.

Cleavage of Tether. Finally, it was necessary to verify that the tethers are really "disposable" and that they can be cleaved after the intramolecular reaction. This was readily accomplished by reduction with LiAlH₄.²⁷ Thus, **7** and **8** afforded diols **10** and **11** in high yield, respectively, Scheme 5.

(25) Salomon, R. G.; Kochi, J. K. *Am. Chem. Soc.* **1973**, *95*, 1889.

(26) In general, the compounds with an alkyl chain as the tether did not form crystals. Only **7d** was crystallized and the crystals were extremely small.

(27) Standard acidic or basic hydrolysis of the esters led to decomposition products.



Conclusions. In summary, we have described a synthetic methodology for the formation of photodimers of *endo*-dicyclopentadienes, notably the previously unknown *syn*-fused isomers. The reaction is highly stereo- and regioselective and the configuration of the cyclobutane rings (either *syn* or *anti*) can be controlled. Finally, adamantyl-containing tethers provided the best results and may prove to be particularly useful linkers in future studies. We are now extending this study to different polycyclic alkenes and dienes to establish whether these results can be generalized.

Experimental Section

General Methods. NMR spectra were obtained on a Varian INOVA 500 spectrometer operating at 499.90 MHz for ^1H and 124.98 MHz for ^{13}C and collected at ambient probe temperature in CDCl_3 , unless otherwise specified. ^1H spectra were referenced to internal tetramethylsilane and ^{13}C spectra to the central line of the solvent. Chemical shifts are reported to a precision of ± 0.01 ppm for proton and ± 0.1 ppm for carbon. Proton coupling constants (J) are reported to a precision of ± 0.1 Hz. High-resolution mass spectral data were obtained from a commercial facility (the Michigan State University Mass Spectrometry Facility). Elemental microanalytical data have been obtained from a commercial facility (Robertson Microlit Laboratories, Inc., Madison, NJ). Low-resolution mass spectra were obtained on a GC/MS HP6890 connected to a HP5973 MSD detector (EI); major ions are reported to unit mass and their intensities are reported parenthetically as a percentage of the strongest peak. Melting points were determined by DSC and the thermograms were performed on a Perkin-Elmer Pyris 1 (scan rate = $10^\circ\text{C}/\text{min}$). 1,3-Adamantane diacetic acid, 1,3-Adamantane dicarboxylic acid, Copper(I)-trifluoromethanesulfonate benzene complex (CuOTf) $_2\cdot\text{C}_6\text{H}_6$, oxalyl chloride and anhydrous pyridine were purchased from Aldrich. Diacid chlorides **2a–d** were directly purchased by Aldrich or Acros, or prepared from the commercially available α,ω diacids and oxalyl chloride as indicated below. Anhydrous THF (Aldrich) was distilled from sodium/benzophenone immediately prior to use. Benzene was dried by removal of water azeotrope and distillation over sodium. Column chromatography was performed using silica gel (Selecto Silica Gel 230–600 mesh). In each case, the crude product was first purified by elution through a first short column, and the purified products mixture was then separated using a long (about 30 cm), thin (1.3 cm internal diameter) column. TLC was performed using Whatman silica gel plates, using iodine and/or a 10% ethanolic solution of phosphomolybdic acid as the developing agents. All reactions were performed under a nitrogen atmosphere in rigorously dry glassware (oven-dried and/or flamed under vacuum).

General Procedure for Preparation of Diesters 3a–f. To a stirred solution of the diacid **2a,b** (1.2 mmol) in benzene (2 mL) was added pyridine (0.2 mL). To this solution was added oxalyl chloride (0.3 mL, 4 mmol) in benzene (1 mL), and the resulting mixture was heated to reflux for 30 min. Benzene was distilled off, and any residual oxalyl chloride was removed in vacuo. The resulting acid chloride was dissolved in benzene (3 mL) and transferred to a flask containing an ice-cold

solution of alcohol **1**¹² (3.3 mmol) in benzene (15 mL) and pyridine (1 mL) under nitrogen atmosphere. After the addition was complete, the mixture was heated to reflux, with stirring, for about 10 h. The reaction mixture was cooled to room temperature and diluted with benzene. The organic layer was washed with 10% HCl (aq), water, and brine and then dried over Na_2SO_4 . The solvent was removed in vacuo to afford a crude oil. Column chromatography (silica gel, hexane/ethyl acetate, 100–95/0–5 v/v depending on the product) afforded pure **3** as a (*R,R/S,S*) and (*R,S/S,R*) diastereomeric mixture in 75–80% yields. **3a**: colorless oil; ^1H NMR δ 6.16 (m, 4H), 5.09 (m, 2H), 3.00 (m, 2H), 2.84 (m, 4H), 2.69 (m, 6H), 1.81 (m, 2H), 1.53–1.64 (m, 4H), 1.32–1.40 (m, 6H). ^{13}C NMR δ 172.1, 137.5, 134.1, 77.6, 52.0, 49.1, 46.7, 45.7, 44.5, 32.6, 29.3, 24.3; HRMS (FAB) calcd for $\text{C}_{24}\text{H}_{30}\text{O}_4$ 382.4710, found (MH^+) 383.5221. **3b**: colorless oil; ^1H NMR δ 6.10 (m, 4H), 5.02 (m, 2H), 2.95 (m, 2H), 2.79 (m, 2H), 2.74 (m, 2H), 2.63 (m, 2H), 2.39 (t, 2H, $J = 7.5$ Hz), 1.98 (m, 2H), 1.76 (m, 2H), 1.42–1.62 (m, 6H), 1.28–1.37 (m, 6H); ^{13}C NMR δ 172.6, 137.2, 134.0, 77.2, 51.9, 49.0, 46.8, 45.6, 44.4, 33.4, 32.6, 24.2, 20.2; HRMS (FAB) calcd for $\text{C}_{25}\text{H}_{32}\text{O}_4$ 396.4976, found (MH^+) 397.2392. **3c**: colorless oil; ^1H NMR δ 6.11 (m, 4H), 5.06 (m, 2H), 2.95 (m, 2H), 2.82 (m, 2H), 2.76 (m, 2H), 2.65 (m, 2H), 2.38 (m, 4H), 1.80 (m, 2H), 1.72 (m, 4H), 1.50 (m, 4H), 1.39 (m, 4H), 1.30 (m, 2H); ^{13}C NMR δ 172.5, 137.4, 134.1, 77.2, 52.0, 49.1, 47.0, 45.7, 44.5, 34.2, 32.7, 24.5, 24.3; HRMS (FAB) calcd for $\text{C}_{26}\text{H}_{34}\text{O}_4$ 410.5242, found (MH^+) 411.2554. **3d**: (*R,R/S,S*) diastereomer; ^1H NMR δ 6.06 (m, 4H), 4.97 (m, 2H), 2.92 (m, 2H), 2.76 (m, 2H), 2.69 (m, 2H), 2.59 (m, 2H), 2.26 (t, 4H, $J = 7.5$ Hz), 1.72 (m, 2H), 1.41–1.62 (m, 8H), 1.24–1.36 (m, 12H); ^{13}C NMR δ 173.3, 137.3, 134.0, 77.1, 52.0, 49.1, 46.9, 45.7, 44.5, 34.3, 32.7, 28.7, 24.8, 24.3; HRMS (FAB) calcd for $\text{C}_{28}\text{H}_{38}\text{O}_4$ 438.5773, found (MH^+) 439.2834. Anal. Calcd for $\text{C}_{28}\text{H}_{38}\text{O}_4$: C, 76.68; H, 8.73. Found: C, 76.61; H, 8.75. **3e**: (*R,R/S,S*) diastereomer: mp 145–146 $^\circ\text{C}$; ^1H NMR δ 6.12 (m, 4H), 5.02 (m, 2H), 2.93 (m, 2H), 2.79 (m, 4H), 2.64 (m, 2H), 2.07–2.12 (m, 6H), 1.78 (m, 2H), 1.50–1.62 (m, 16H), 1.30–1.39 (m, 4H); ^{13}C NMR δ 171.5, 137.5, 134.1, 76.9, 52.1, 49.1, 48.6, 47.4, 47.0, 45.9, 44.7, 41.4, 35.7, 33.3, 32.8, 28.8, 24.4; HRMS (FAB) calcd for $\text{C}_{32}\text{H}_{44}\text{O}_4$ 516.3240, found (MH^+) 517.3314. Anal. Calcd for $\text{C}_{32}\text{H}_{44}\text{O}_4$: C, 79.03; H, 8.58. Found: C, 78.24; H, 8.48. **3f**: mp 172–173 $^\circ\text{C}$; ^1H NMR δ 6.16 (m, 4H), 5.06 (m, 2H), 3.0 (m, 2H), 2.86 (m, 2H), 2.79 (m, 2H), 2.55 (m, 2H), 2.23 (m, 2H), 2.10 (m, 2H), 1.95 (m, 8H), 1.80 (m, 2H), 1.75 (m, 2H), 1.48 (m, 4H), 1.49 (m, 4H), 1.31 (m, 2H); ^{13}C NMR δ 176.7, 137.5, 134.3, 77.2, 51.8, 48.9, 47.1, 45.7, 44.3, 40.9, 40.1, 38.1, 35.4, 32.5, 27.9, 24.2; HRMS (FAB) calcd for $\text{C}_{32}\text{H}_{40}\text{O}_4$ 488.2927, found (MH^+) 489.2991. Anal. Calcd for $\text{C}_{32}\text{H}_{40}\text{O}_4$: C, 78.65; H, 8.25. Found: C, 78.58; H, 8.31.

Intermolecular Photocycloaddition of 4. A 50 mg portion of **4** (0.3 mmol) was dissolved in dry THF (30 mL) and put in a quartz tube shielded by a Vycor filter. A catalytic amount (about 5–8 mol %) of (CuOTf) $_2\cdot\text{C}_6\text{H}_6$ was added, and the tube was closed with a septum and the solution was irradiated with a 450 W Hanovia medium-pressure Hg lamp placed in a quartz well. The well was positioned at 3 cm distance from the quartz tube containing the solution. The reaction was monitored by GC/MS. After 56h the solvent was removed under reduced pressure and the products were separated by silica gel column chromatography (hexane/ethyl acetate, 98/2) and recrystallized from hexane. The total yield of **5** and **6** is 62% (31 mg) and the ratio of **5**:**6** was 1:1. **5**: mp 180–182 $^\circ\text{C}$; MS m/z 328 (M^+ , 25), 197 (55), 164 (46), 132 (100), 129 (75), 67 (85); ^1H NMR δ 3.74 (m, 2H), 3.36 (s, 6H), 2.36 (m, 2H), 2.28 (m, 2H), 2.21 (d, 2H, $J = 5.5$ Hz), 2.15 (d, 2H, $J = 10.0$ Hz), 2.06 (d, 2H, $J = 4.0$ Hz), 2.01 (d, 2H, $J = 5.0$ Hz), 1.85 (m, 4H), 1.55 (m, 2H), 1.38 (m, 4H), 1.32 (d, 2H, $J = 10.0$ Hz); ^{13}C NMR δ 84.5, 57.9, 45.2, 44.1, 42.7, 42.0, 40.2, 38.6, 37.4, 32.7, 22.7. **6**: mp 125–127 $^\circ\text{C}$; MS m/z 328 (M^+ , 26), 197 (75), 164 (43), 132 (95), 129 (100), 67 (96); ^1H NMR δ 3.74 (m, 2H), 3.36 (s, 6H), 2.34 (m, 2H), 2.28 (m, 2H), 2.21 (d, 2H, $J = 5.5$ Hz), 2.15 (d, 2H, $J = 10.0$ Hz), 2.11 (d, 2H, $J = 4.5$ Hz), 1.95 (d, 2H, $J = 5.0$ Hz), 1.83 (m, 4H), 1.55 (m, 2H),

1.38 (m, 4H), 1.31 (d, 2H, $J = 10.0$ Hz); ^{13}C NMR δ 84.5, 57.9, 45.0, 44.1, 42.7, 42.1, 40.8, 38.1, 37.4, 32.7, 22.7.

General Procedure for [2 + 2] Intramolecular Photocycloadditions. The photocycloaddition conditions were optimized for each diester by first performing the reaction in a quartz NMR tube with THF- d_6 and monitoring by ^1H NMR spectroscopy. Each reaction was then repeated on a larger scale as follows. Diester **3** (0.1 mmol) was dissolved in dry THF (20 mL) and placed in a dry quartz tube shielded with a Vycor filter. A catalytic amount (about 5 mol %) of $(\text{CuOTf})_2 \cdot \text{C}_6\text{H}_6$ was added and the solution was irradiated with a 450 W Hanovia medium-pressure Hg lamp placed in a quartz well. The well was positioned at 2–3 cm distance from the quartz tube containing the solution. The reaction was monitored by TLC and ^1H NMR spectroscopy (disappearance of olefinic protons). After the reaction was complete, THF was removed in vacuo and the crude residue purified by silica gel column chromatography (silica gel, hexane/ethyl acetate, 100–95/0–5 v/v depending on the product) to afford pure **7** and **8**.²⁸ **7b**: mp 116–118 °C; ^1H NMR δ 5.08 (m, 2H), 2.76 (m, 2H), 2.46 (m, 4H), 2.44 (m, 6H), 2.28 (m, 4H), 2.07–2.17 (m, 6H), 2.00 (m, 2H), 1.80 (m, 2H), 1.64 (m, 2H), 1.48 (m, 4H); ^{13}C NMR δ 173.4, 79.6, 50.2, 44.3, 42.3, 39.7, 38.4, 37.4, 34.7, 34.6, 21.8, 20.8; HRMS (FAB) calcd for $\text{C}_{25}\text{H}_{32}\text{O}_4$ 396.4976, found (MH⁺) 397.2391. **8b**: mp 95–97 °C; ^1H NMR δ 5.00 (m, 2H), 3.23 (m, 2H), 2.87 (m, 2H), 2.58 (m, 4H), 2.37 (m, 4H), 2.13–2.34 (m, 6H), 1.96–2.06 (m, 8H), 1.57 (m, 2H), 1.41 (m, 4H); ^{13}C NMR δ 172.6, 78.0, 50.4, 48.3, 44.6, 42.3, 41.5, 39.9, 37.8, 36.0, 35.7, 23.3, 22.5; HRMS (FAB) calcd for $\text{C}_{25}\text{H}_{32}\text{O}_4$ 396.4976, found (MH⁺) 397.2393. **7c**: mp 120–121 °C; ^1H NMR δ 4.87 (m, 2H), 2.84 (m, 2H), 2.41 (m, 2H), 2.35 (m, 2H), 2.26 (m, 2H), 2.17 (d, 2H, $J = 9.5$ Hz), 2.14 (m, 2H), 2.03–2.09 (m, 6H), 1.75–1.82 (m, 6H), 1.58–1.69 (m, 4H), 1.43–1.51 (m, 4H); ^{13}C NMR δ 174.2, 79.6, 46.8, 43.6, 43.3, 42.9, 39.4, 38.4, 37.0, 36.0, 33.2, 37.5, 28.0, 22.6, 21.7, 14.1; HRMS (FAB) calcd for $\text{C}_{26}\text{H}_{34}\text{O}_4$ 410.5242, found (MH⁺) 411.2549. **8c**: mp 110–112 °C; ^1H NMR δ 4.85 (m, 2H), 2.99 (m, 2H), 2.79 (m, 2H), 2.66 (m, 2H), 2.56 (d, 2H, $J = 11.0$ Hz), 2.32–2.39 (series of m, 6H), 2.20 (d, 2H, $J = 5.0$ Hz), 2.10 (d, 2H, $J = 4.0$ Hz), 1.99 (m, 2H), 1.93 (m, 2H), 1.65–1.73 (m, 4H), 1.55 (m, 2H), 1.41 (m, 4H); ^{13}C NMR δ 172.8, 49.8, 47.3, 42.7, 42.4, 41.6, 41.1, 39.0, 35.5, 35.2, 25.7, 22.4; HRMS (FAB) calcd for $\text{C}_{26}\text{H}_{34}\text{O}_4$ 410.5242, found (MH⁺) 411.2538. **7d**:²⁸ ^1H NMR δ 4.93 (m, 2H), 2.67 (m, 2H), 2.50 (m, 2H), 2.35 (m, 2H), 2.17 (m, 4H), 2.09 (m, 2H), 2.01 (m, 2H), 1.85–1.93 (m, 6H), 1.60–1.67 (m, 8H), 1.37–1.42 (m, 8H); ^{13}C NMR δ 173.3, 77.6, 45.3, 43.9, 43.0, 42.1, 40.4, 38.3, 37.2, 36.1, 32.2, 29.6, 26.0, 22.0; HRMS (FAB) calcd for $\text{C}_{29}\text{H}_{38}\text{O}_4$ 438.5773, found (MH⁺) 439.2834. **7e**:²⁸ mp slow decomposition above 300 °C; ^1H NMR δ 4.72 (m, 2H), 2.76 (m, 2H), 2.43 (d, 2H, $J = 12.5$ Hz), 2.38 (m, 2H), 1.89–2.16 (series of m, 20H), 1.58–1.66 (m, 6H), 1.40–1.49 (m, 10H); ^{13}C NMR δ 171.3, 78.7, 47.8, 46.0, 44.5, 44.0, 43.8, 43.7, 40.0, 39.6, 38.7, 37.3, 36.3, 34.3, 33.8, 28.6, 21.9; HRMS (FAB) calcd for $\text{C}_{34}\text{H}_{44}\text{O}_4$ 516.3240, found (M⁺) 517.3214 (–2.6 m), found (MH⁺) 517.3304. **7f**: mp: slow decomposition above 300 °C; ^1H NMR δ 5.12 (m, 2H), 2.77 (m, 2H), 2.43 (m, 2H), 2.35 (d, 2H, $J = 5.0$ Hz), 2.22 (d, 2H, $J = 10.0$ Hz), 2.13–2.18 (m, 4H), 2.10 (m, 2H), 1.98–2.06 (m, 8H), 1.88 (m, 4H), 1.65–1.71 (m, 8H), 1.50–1.56 (m, 2H), 1.36 (d, 2H, $J = 10.0$ Hz); ^{13}C NMR δ 172.3, 79.7, 49.9, 44.5, 43.6, 43.1, 42.1, 40.8, 39.0, 38.9, 37.7, 37.4, 36.6, 35.5, 33.9, 28.3, 21.3; HRMS (FAB) calcd for $\text{C}_{32}\text{H}_{40}\text{O}_4$ 488.2927, found (MH⁺) 489.3005. **8f**: mp slow decomposition above 300 °C; ^1H NMR δ 5.03 (m, 2H), 3.18 (m, 2H), 2.89 (m, 2H), 2.58 (m, 6H), 2.40 (m, 2H), 1.97–2.22 (m, 10H), 1.91 (m, 2H), 1.71–1.78 (m, 6H), 1.61 (m, 2H), 1.37–1.44 (m, 6H); ^{13}C NMR δ 176.2, 78.0, 50.8, 48.5, 45.1, 42.1, 42.0, 39.9, 38.8, 37.2, 36.8, 35.8, 29.6, 28.4, 28.3, 22.5; HRMS (FAB) calcd for $\text{C}_{32}\text{H}_{40}\text{O}_4$ 488.2927, found (MH⁺) 489.3012. Mixture of **7f** and **8f**. Anal. Calcd for $\text{C}_{32}\text{H}_{40}\text{O}_4$: C, 78.65; H, 8.25. Found: C, 79.43; H, 9.59.

General Procedure for Cleavage of the Tether. LiAlH_4 (0.06 mmol) was suspended in THF (1 mL) and cooled with an ice bath. To this stirred suspension was added dropwise a solution of **7d,e** or **8c,f** (0.03 mmol) in THF (2 mL). After the addition was complete, the contents were allowed to warm to

room temperature and stirred for another 30 min. Excess LiAlH_4 was cautiously destroyed by dropwise addition of ethyl acetate and 1–2 drops of aqueous Na_2SO_4 satd. solution. The reaction mixture was then extracted with ethyl acetate and washed with water and brine, and the organic layer was dried over Na_2SO_4 . The solvent was removed in vacuo to yield a solid residue which was purified by column chromatography (hexane/ethyl acetate, 60/40 v/v) to obtain pure **10** (from **7d,e**) or **11** (from **8c,f**) (7 mg, 84% yield) as a crystalline solid. **10**: mp 202–204 °C; ^1H NMR δ 4.22 (m, 2H), 3.09 (m, 2H), 2.79 (m, 2H), 2.66 (d, 2H, $J = 11$ Hz), 2.36 (m, 6H), 2.23 (m, 2H), 2.00 (m, 2H), 1.55–1.66 (m, 6H), 1.41 (m, 2H), 1.36 (d, 2H, $J = 11$ Hz); ^{13}C NMR δ 75.1, 49.9, 45.2, 42.5, 42.3, 41.9, 41.1, 40.1, 36.4, 22.6. HRMS (FAB) calcd for $\text{C}_{20}\text{H}_{28}\text{O}_2$ 300.2089, found (M⁺) 300.2029 (0.3 m); (MH⁺) 301.2161 (–0.7 m); (M–1) 299.2009. **11**: mp 190–192 °C; ^1H NMR δ 4.22 (m, 2H), 3.09 (m, 2H), 2.79 (m, 2H), 2.66 (d, 2H, $J = 10.5$ Hz), 2.36 (m, 6H), 2.23 (m, 2H), 1.92 (m, 2H), 1.55–1.66 (m, 6H), 1.41 (m, 2H), 1.36 (d, 2H, $J = 11$ Hz); ^{13}C NMR δ 75.1, 49.9, 45.2, 42.5, 42.3, 41.9, 41.1, 40.1, 36.4, 22.6; HRMS (FAB) calcd for $\text{C}_{20}\text{H}_{28}\text{O}_2$ 300.2089, found (M⁺) 300.2097.

Experimental Crystal Data. Intensity data were measured on a Bruker diffractometer with $\text{CuK}\alpha$ radiation ($\lambda = 1.54178$ Å). Structures were solved by direct methods, aided by program XS, and refined with full-matrix least-squares program XL, from SHELXTL.²⁹ The XL program minimizes F^2 differences, and uses *all* data; i.e., weak data are not considered “unobserved” during refinement. For **5**: $\text{C}_{22}\text{H}_{32}\text{O}_2$, FW = 328.48, triclinic space group $P(-1)$; $a = 6.9036(3)$ Å, $b = 7.6249(4)$ Å, $c = 8.9770(7)$ Å, $\alpha = 87.060(7)^\circ$, $\beta = 70.192(5)^\circ$, $\gamma = 78.226(5)^\circ$, $V = 435.15(5)$ Å³, $Z = 1$, and $D(\text{X-ray}) = 1.253$ mg mm⁻³. 1589 data measured to a 2θ max of 115° at $T = 294$ K. $R = 0.0359$ for 1157 reflections with $[I > 2\sigma(I)]$, $R = 0.0367$, $wR2 = 0.1017$ for *all* 1192 unique reflections. For **6**: $\text{C}_{22}\text{H}_{32}\text{O}_2$, FW = 328.48, triclinic space group $P(-1)$; $a = 7.7130(4)$ Å, $b = 8.9995(7)$ Å, $c = 13.5820(9)$ Å, $\alpha = 106.814(6)^\circ$, $\beta = 92.935(7)^\circ$, $\gamma = 96.154(6)^\circ$, $V = 893.9(1)$ Å³, $Z = 2$, and $D(\text{X-ray}) = 1.220$ mg mm⁻³. 2718 data measured to a 2θ max of 115.5° at $T = 294$ K. $R = 0.0572$ for 2320 reflections with $[I > 2\sigma(I)]$, $R = 0.0586$, $wR2 = 0.1521$ for *all* 2444 unique reflections. For **7e**: $\text{C}_{34}\text{H}_{44}\text{O}_4$, FW = 516.69, monoclinic space group $C2/c$; $a = 35.4020(13)$ Å, $b = 7.7641(4)$ Å, $c = 19.7431(5)$ Å, $\beta = 100.14(1)^\circ$, $V = 5342.0(4)$ Å³, $Z = 8$, and $D(\text{X-ray}) = 1.285$ mg mm⁻³. 4287 data measured to a 2θ max of 116° at $T = 294$ K. $R = 0.0541$ for 2443 reflections with $[I > 2\sigma(I)]$, $R = 0.088$, $wR2 = 0.1359$ for *all* 3482 unique reflections. This crystal was twinned by a rotation about the real c axis. The crystal shape is a thin lath or sword, with the major face indexed as the 100. Twinning is caused by stacking of thin lathes that occasionally differed by 180 degrees in the direction of their $+b$ long axes, a reasonable stacking fault. The $hk0$ layers of the two twin diffraction patterns are exactly superimposed. This was partially corrected by assigning, and refining, a separate scale factor for the $hk0$ data. The $l = 3$ layer had to be excluded from the refinement, because the two patterns almost coincide, and reflections overlap, on that level. Thirteen reflections from other layers were excluded for likely twin interference; all had large discrepancies of the $F_o \gg F_c$ type. Several crystals were examined and all were twinned but the volume-ratio of the two components varied. In the best case, reported herein, the V ratio was about 3:1. For **8f**: $\text{C}_{32}\text{H}_{40}\text{O}_4$, FW = 488.64, monoclinic space group $P2_1/c$; $a = 6.4064(4)$ Å, $b = 18.637(1)$ Å, $c = 20.683(1)$ Å, $\beta = 95.31(1)^\circ$, $V = 2458.9(3)$ Å³, $Z = 4$, and $D(\text{X-ray}) = 1.320$ mg mm⁻³. 7662 data measured to a 2θ max of 116° at $T = 294$ K. $R = 0.0499$ for 2754 reflections with $[I > 2\sigma(I)]$, $R = 0.0627$, $wR2 = 0.1290$ for *all* 3424 unique reflections.

More details, structural results and figures for **5**, **6**, **7e**, and **8f** are reported in the Supporting Information and have been deposited with the Cambridge Crystallographic Data

(28) Compounds **8d** and **8e** have not been synthesized, because the photocycloadditions of **3d** and **3e** were performed on the isolated (R, R/S, S) diastereomer, which produces only the exo-trans-exo isomer **7**.
(29) Shelldrick, G. SHELXTL96, *Acta Crystallogr. A* **1990**, *46*, 467.

Centre. Copies can be obtained from Director, CCDC, 12 Union Road, Cambridge CB2 1EZ, UK (e-mail: deposit@ccdc.cam.ac.uk).

Acknowledgment. E.G. thanks Prof. William Dailley, Prof. Kurt Deshayes, and Prof. Andrea Lazzeri for insightful discussions and the Rutgers University Research Council for financial support. R.G. is grateful for the support of the Office of Naval Research.

Supporting Information Available: X-ray structural information on **5**, **6**, **7e**, **8f** including tables of atomic coordinates, bond lengths and angles, anisotropic displacement parameters, hydrogen coordinates, a description of the observed X-ray-induced rearrangement of **8f** and 15 figures. This material is available free of charge via the Internet at <http://pubs.acs.org>.

JO0055990